Materials Science and Engineering B107 (2004) 237–240

www.elsevier.com/locate/mseb

Effect of rapid thermal annealing on beryllium implanted p-type GaN

Hung Wen Huang [a], C.C. Kao [a], J.Y. Tsai [a], C.C. Yu [a], C.F. Chu [a], J.Y. Lee [a], S.Y. Kuo [a], C.F. Lin [a], H.C. Kuo [b,*], S.C. Wang [a]

[a] *Institute of Electro-Optical Engineering, National Chiao Tung University, Hsinchu 30050, Taiwan, ROC*
[b] *Precision Instrument Development Center, Taiwan*

Received 11 March 2003; accepted 12 April 2003

Abstract

We report the results of rapid thermal annealing (RTA) effect on beryllium implanted in situ activated p-type GaN samples and investigate the ramping and isothermal annealing effect of RTA process for these samples. It is found that the optimum RTA condition is at the temperature of 1100 °C for 15 s. Furthermore, with equal total isothermal time of 60 s, we compared the multiple step annealing (MSA) at 1100 °C for four periods with single step annealing (SSA) for one period at the same annealing temperature of 1100 °C, and observed that the ramping effect with MSA could repair Be-related complex defect, and one time, long period isothermal annealing effect with SSA seems to induce much more defect. It seems that the multiple step annealing is more effective and induce less defect than single step annealing for Be-implanted in situ activated p-type GaN samples.

Keywords: RTA; Beryllium; Implantation; GaN; SSA; MSA

Gallium nitride and other group III-nitrides materials have recently attracted large interest for opto-electronic device such as blue-green light-emitting diodes, laser diodes and detectors [1–4]. Most of these devices have been made by the achievement of controlled p-type and n-type doping during metal-organic chemical vapor deposition (MOCVD) process [5–11]. Ion implantation for selective area doping is a critical requirement in the semiconductor industry because of its wide acceptance and providing precise control of dopant concentration and depth distribution. However, the implantation-induced damage removal and efficient activation of both p-type and n-type dopants are important and usually performed by the technology of rapid thermal annealing (RTA) [12–14]. Generally, p-type GaN is typically achieved by doping with magnesium (Mg). Because of high activation energy of Mg [15–17], the activation of Mg acceptors is generally very low and limited to less than 10%. Be has a low theoretical activation energy of about 60 meV [18] making it a promising candidate for p-type doping in GaN. Several studies have indicated that the activation of Be implanted undoped GaN dopants can be achieved by rapid thermal annealing up to 1100 °C [19,20], including different annealing methods. Recently, Be-implanted Mg doped GaN have been reported and obtained very high hole concentration over $10^{19}\,cm^{-3}$ and low specific resistance [21–24]. However, there is no systematic examination of implantation-induced damages and the detail effect of RTA on Be implanted in situ activated p-type GaN materials. In this paper, we report the effect of different RTA approaches of single step annealing (SSA) and multiple step annealing (MSA) on Be-implanted in situ activated p-type GaN including electrical and optical properties, and also demonstrate the ramping and the isothermal annealing effect of RTA process on these p-type GaN samples.

The in situ activated p-type GaN samples were 1 μm-thick, grown on *c*-axis sapphire substrates by MOCVD. Trimethlygallium, ammonia and CP_2Mg were used as Ga, N and Mg source, respectively. These in situ activated p-type GaN samples were not treated by post-growth annealing and activated in situ in the reactor of MOCVD instrument. The initial hole concentration and mobility at room temperature for these in situ activated samples prior to Be implantation were measured by Hall measurement to be $1.2 \times 10^{17}\,cm^{-3}$ and $13\,cm^2/V\,s$, respectively. These samples were subsequently implanted with Be ions at the energies of 50 keV with a dose of $10^{14}\,cm^{-2}$. The carrier concentration of these samples

* Corresponding author. Tel.: +886-3-5712121x31986; fax: +886-3-571-6631.
E-mail address: hckuo@faculty.nctu.edu.tw (H.C. Kuo).

0921-5107/$ – see front matter © 2004 Elsevier B.V. All rights reserved.
doi:10.1016/j.mseb.2003.12.001

was determined by Hall measurement at room temperature. The photoluminescence (PL) measurements were obtained at a temperature of 20 K using a He–Cd laser as the excitation source. The strains of these samples were characterized by the Raman analysis system and the X-ray diffraction experiments were performed using a high-resolution X-ray diffractometer with the Cu Kβ ($\lambda = 1.541$ A) line.

As shown in Fig. 1, the ion projection range of implantation energy 50 keV for as-implant samples was estimated to be about 0.25 μm by TRIM stimulation and observed to be about 0.4 μm from SIMS measurement. It has been shown that the profile of ions is similar but the depth is not equal. The typical reason is that TRIM simulation value is based on undoped GaN. These implanted samples were subsequently separated into two sets for different RTA approaches. The first set was with SSA at 1100 °C for 60 s of one period, while the second set was with MSA for 15 s of four periods at the same annealing temperature of 1100 °C, to repair the implantation damage.

The hole carrier concentration and mobility of the second set samples with MSA were measured by Hall measurement to be 4.0×10^{17} cm^{-3} and 13 cm^2/V s, respectively, while for the first set samples with SSA, the value of the carrier concentration could not be obtained because of very high resistance. It is clearly shown that the carrier concentration of the second set with MSA has a little increase than the as-grown samples.

Using a 325 nm He–Cd laser as excitation source, these two set samples were characterized by PL measurement. The PL spectra of the first set and second samples as shown in Fig. 2, shows several typical Mg-related emission lines at 420, 440 and 465 nm. The 420 and 440 nm peak are attributed to donor–acceptor-pair transitions from the deeper donors to the identical shallow acceptor. Additionally, a deeper Mg-related acceptor level of about 530 meV from the valence band and thus 465 nm transition is considered

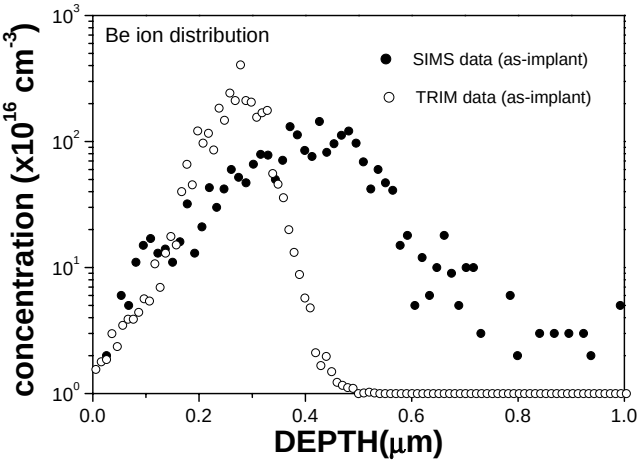

Fig. 1. The Be ion projection range of energy 50 keV for as-implant samples was estimated to be about 0.25 μm by TRIM stimulation and observed to be about 0.4 μm from SIMS measurement.

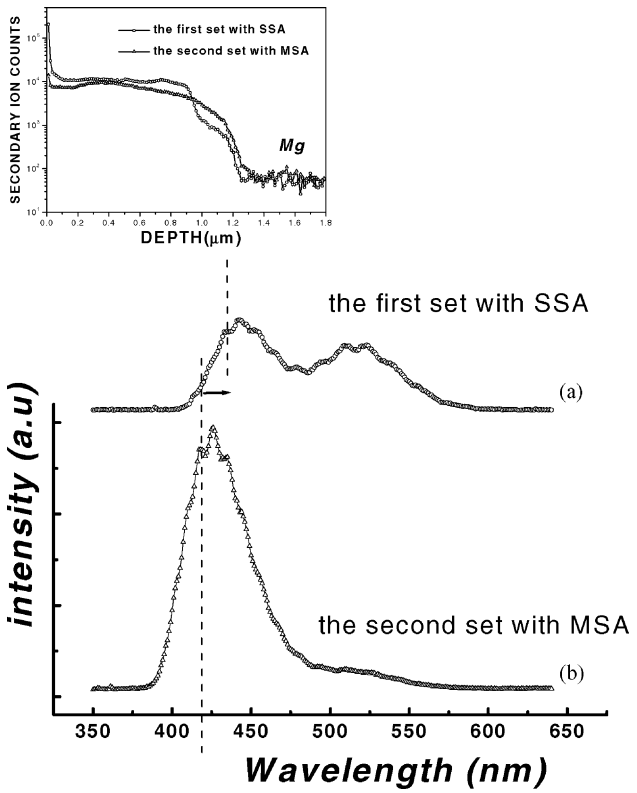

Fig. 2. The PL spectra of (a) the first set with SSA and (b) the second set with MSA. Inset diagram indicates occurrence of partial accumulation of Mg atoms.

to be due to randomly dispersed deep acceptors, defects and impurities such as V_{ga}, V_N, Mg_{Ga}, O_N and Mg-complexes [25,26]. The PL spectra show an additional broad spectrum near 520 nm which is Be-related complex defect induced by ion implantation [26]. From Fig. 2 in the first set with SSA, the Mg-related emission lines intensity is much weaker and Be-related complex defect at 520 nm was obviously compared to the second set with MSA. This suggests that the several ramping effect of MSA could repair Be-related complex defect, however, one time, long period isothermal annealing effect with SSA seems to be inducing much more defect. Furthermore, we could observe that the Mg-related emission lines of the first set are obviously red-shifted compared to the second set, indicating occurrence of partial accumulation of Mg atoms [27]. As shown in Fig. 2, in the insert diagram, the SIMS profiles of Mg in the first set and the second set are comparable. To further simulate the thermal redistribution of Be ion for SSA and MSA, we combined the ion approximated Gaussian distribution equation and diffusion equation, and obtain the implanted annealing distribution equation, which has the form of

$$n(x) = \frac{S}{\sqrt{2\pi}\sqrt{\Delta R_p^2 + 2Dt}} \exp\left[-\frac{1}{2}\left(\frac{x - R_p}{\sqrt{\Delta R_p^2 + 2Dt}}\right)^2\right]$$

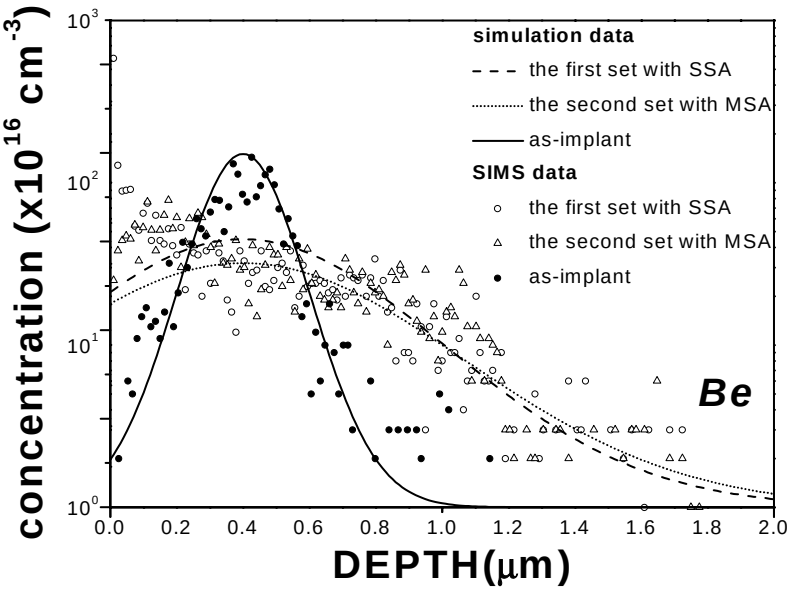

Fig. 3. The distribution of Be ions of these two set samples from simulation and SIMS.

where S is the total dose, R_p the ion projection range, ΔR_p the ion projection straggle, D the diffusion coefficient, and t the annealing time. Fig. 3 show the distribution of Be ions of these two set of samples from simulation and SIMS. We obtain the same profile about the simulation and SIMS data, and the redistribution of Be ions in p-type film with SSA and MSA is uniform.

Meanwhile, we implement the comparison of X-ray diffraction measurement data between the first set and the second set samples. The X-ray diffraction experiments were performed using a high resolution X-ray diffractometer with the Cu Kβ ($\lambda = 1.541$ A) line. From the full width half maximum value of X-ray rocking curve (XRC) spectra, it can be seen that the crystal quality of the first set for SSA with the value of about 442 arcsec is worst than that of the second set for MSA with the value of about 412 arcsec. This also could prove that one time, long period isothermal annealing would result in much more defects. To further investigate the ramping and isothermal effect on Be-implanted p-type GaN, we measured the Raman spectrum of the first set and second set as shown in Fig. 4. From the Raman spectra, the peaks at about 414 and 746 cm^{-1} are the A_{1g} and E_{1g} modes arising from the substrates, and the peak at 375 cm^{-1} is also assigned to arise from the substrate [28,29]. From Fig. 4, in the Raman spectrum of the first set, we can observe the E_2 (high) mode of GaN at about 567 cm^{-1} is higher than the second set of 565 cm^{-1}. This suggests is indicated that the several ramping effects of MSA are more effective to relax the residual strain. This results is consistent with the X-ray XRC measurements.

In summary, we have realized the study of rapid thermal annealing effect on beryllium implanted into in situ activated p-type GaN samples, and investigated the ramping and the isothermal annealing effect of RTA process. We compared the multiple step annealing at 1100 °C for 15 s of four periods with single step annealing for 60 s of one period at the same annealing temperature, and observed that the ramping effect with MSA could repair Be-related complex defect and one time, long period isothermal annealing effect with SSA seems to be inducing much more defect. It seems that the multiple step annealing is more effective and induces less defect than single step annealing for Be-implanted in situ activated p-type GaN samples.

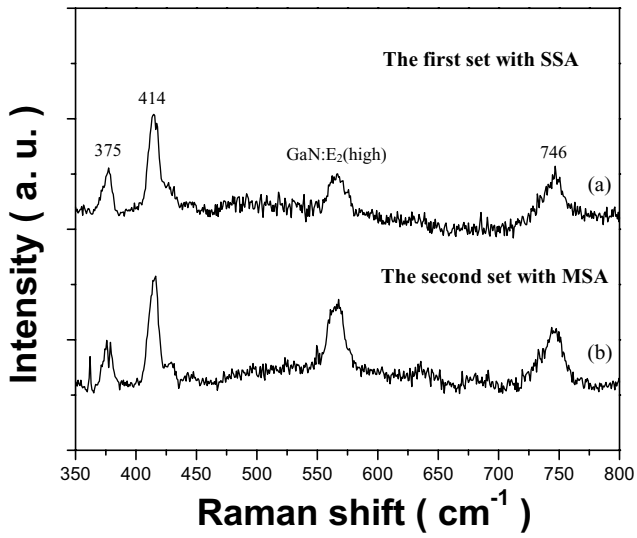

Fig. 4. Raman spectra of Be-implanted in situ activated p-type GaN samples with SSA and MSA at the same annealing temperature of 1100 °C: (a) the first set with SSA and (b) the second set with MSA.

Acknowledgements

This work was supported in part by National Science Council of Republic of China (ROC) in Taiwan under contract No. NSC 92-2215-E-009-015 and by the Academic Excellence Program of the ROC Ministry of Education under the contract No. 88-FA06-AB. The authors would like to thank Dr. G.C. Chi of National Central University (NCU) for the use of the ion implantation facility.

References

[1] S. Nakamura, T. Mokai, M. Senoh, Appl. Phys. Lett. 76 (1994) 8189.
[2] S. Nakamura, M. Senoh, S. Nagahama, N. Iwasa, T. Yamada, T. Matsushita, H. Kiyoku, Y. Sugimoto, Jpn. J. Appl. Phys. 35 (1996) L74.
[3] S. Nakamura, M. Senoh, S. Nagahama, N. Iwasa, T. Yamada, T. Matsushita, Y. Sugimoto, H. Kiyodo, Appl. Phys. Lett. 70 (1996) 868.
[4] S. Nakamura, MRS Bull. 22 (1997) 29.
[5] B. Goldenberg, J.D. Zook, R.J. Ulmer, Appl. Phys. Lett. 62 (1993) 381.
[6] M.E. Lin, G. Xue, G.L. Zhou, J.E. Greene, H. Morkoe, Appl. Phys. Lett. 63 (1993) 932.
[7] C. Wang, R.F. Davis, Appl. Phys. Lett. 63 (1993) 990.
[8] J.G. Kim, A.C. Frenkel, H. Liu, R.M. Park, Appl. Phys. Lett. 65 (1994) 91.
[9] R.J. Molnar, T.D. Moustakas, J. Appl. Phys. 76 (1994) 4587.
[10] M. Rubin, N. Newman, J.S. Chan, T.C. Fu, J.T. Ross, Appl. Phys. Lett. 64 (1994) 64.
[11] C.R. Abernathy, J.D. Mackenzie, S.J. Pearton, W.S. Hobson, Appl. Phys. Lett. 66 (1995) 1969.
[12] J.C. Zolper, R.G. Wilson, S.J. Pearton, R.A. Stall, Appl. Phys. Lett. 68 (1996) 1945.
[13] S.J. Pearton, C.B. Vartuli, J.C. Zolper, C. Yuan, R.A. Stall, Appl. Phys. Lett. 67 (1997) 2313.
[14] H.H. Tan, J.S. Williams, J. Zou, D.J.H. Cockayne, S.J. Pearton, J.C. Zolper, R.A. Stall, Appl. Phys. Lett. 72 (1998) 1190.
[15] B. Podor, Semicond. Sci. Technol. 11 (1996) 827.
[16] J.I. Pankove, J.A. Hutchby, J. Appl. Phys. 47 (1976) 5387.
[17] J.W. Orton, Semicond. Sci. Technol. 10 (1995) 101.
[18] F. Bernardini, V. Fiorentini, A. Bosin, Appl. Phys. Lett. 70 (1997) 2990.
[19] C. Ronning, K.J. Linthicum, E.P. Carlson, P.J. Hartlieb, D.B. Thomson, T. Gehrke, R.F. Davis, MRS INTERNET J. N. S. R. 4 (Suppl. 1) (1999) U208–U213.
[20] Y.J. Sun, L.S. Tan, S.J. Chua, S. Prakash, MRS INTERNET J. N. S. R. 5S1 (Suppl. 1) (2000) U270–U275.
[21] C.F. Chu, C.C. Yu, Y.K. Wang, J.Y. Tsai, F.I. Lai, S.C. Wang, Appl. Phys. Lett. 77 (2000) 3423.
[22] C.C. Yu, C.F. Chu, J.Y. Tsai, C.F. Lin, S.C. Wang, Mater. Sci. Eng. B 82 (2001) 82.
[23] C.C. Yu, C.F. Chu, J.Y. Tsai, C.F. Lin, W.H. Lan, C.I. Chiang, S.C. Wang, Jpn. J. Appl. Phys. 40 (2001) L417.
[24] C.C. Yu, C.F. Chu, J.Y. Tsai, C.F. Lin, S.C. Wang, J. Appl. Phys. 92 (2002) 1881.
[25] U. Kaufmann, M. Kunzer, M. Maier, H. Obloh, A. Ramakrishnan, B. Santic, P. Schlotter, Appl. Phys. Lett. 72 (1998) 1326.
[26] P. Boguslawski, E.L. Briggs, J. Bernholc, Phys. Rev. B 51 (1995) 8067.
[27] J.K. Sheu, Y.K. Su, G.C. Chi, B.J. Pong, V.Y. Chen, C.N. Huang, W.C. Chen, J. Appl. Phys. 84 (1998) 4590.
[28] F.A. Ponce, J.W. Steeds, C.D. Dyers, G.D. Pitt, Appl. Phys. Lett. 69 (1996) 2650.
[29] X.B. Li, D.Z. Sun, J.P. Zhang, M.Y. Kong, Appl. Phys. Lett. 72 (1998) 936.